Effect of Encapsulation of Curcumin in Polymeric Nanoparticles (NPs): How Efficient to Control ESIPT Process?

ARTICLE *in* LANGMUIR · AUGUST 2014

Impact Factor: 4.46 · DOI: 10.1021/la5023533 · Source: PubMed

Langmuir

Article

pubs.acs.org/Langmuir

Effect of Encapsulation of Curcumin in Polymeric Nanoparticles: How Efficient to Control ESIPT Process?

Chiranjib Banerjee, Saikat Maiti, Mainak Mustafi, Jagannath Kuchlyan, Debasis Banik, Niloy Kundu, Dibakar Dhara,* and Nilmoni Sarkar*

Department of Chemistry, Indian Institute of Technology, Kharagpur 721302, WB India

Supporting Information

ABSTRACT: This paper demonstrates the photophysics of curcumin inside polymeric nanoparticles (NPs), which are being recently used as targeted drug delivery vehicles. For this purpose, we have prepared three polymeric NPs by ultrasonication method from three well-defined water-insoluble random copolymers. These copolymers having various degrees of hydrophobicity were synthesized via reversible addition−fragmentation transfer (RAFT) method using styrene and three different functional monomers, namely, 2-hydroxyethyl acrylate, 4-formylphenyl acrylate, and 4-vinylbenzyl chloride. The photophysics of the curcumin molecules inside the polymeric NPs have been monitored by applying tools like steady state and time-resolved fluorescence spectroscopy. An increase in fluorescence intensity along with an increase in the lifetime values indicated a perturbation of the excited state intramolecular proton transfer (ESIPT) process of curcumin inside the polymeric NPs.

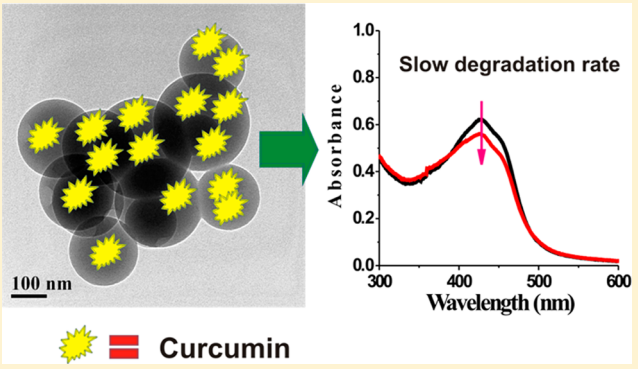

1. INTRODUCTION

The application of nanotechnology to develop medicines that are safer and also more effective is established to substantially influence the landscape of pharmaceutical industries for future generations.[1,2] This is because of the innovations and the emerging successes of drug delivery systems based on nanoparticles (NPs).[3] Polymeric NPs have recently emerged as an effective and powerful therapeutic tool for controlled delivery of different drugs to targeted areas with simultaneous reduction of toxic effects that are otherwise caused by these drugs.[4,5] The advantages also include improving the solubility of water insoluble drugs, sustaining the circulation time of drugs, releasing the drugs at a stable rate which lowers the frequency of administration, and delivering multiple types of drugs simultaneously for combination therapies.[6−8] Although the clinical applications of these nanoparticles still face various problems, like premature release of the encapsulated drugs from the polymeric NPs as well as the stability of the drugs, which are the major obstacles for site specific drug delivery.[9−11] Moreover, it also faces challenges related to the therapeutic effect which includes (1) improvement of pharmaceutical and pharmacological properties of drugs, keeping the drug molecules unaltered, (2) drug delivery across a range of biological barriers including epithelial and endothelial, (3) drug delivery to intracellular sites of action, and (4) the ability to deliver multiple types of therapeutics with potentially different physicochemical properties.[12] In this context, understanding the photophysics of the drug molecules inside the polymeric NPs would be highly beneficial for their medicinal trials.

Curcumin is a yellow pigment of rhizomes present in the plant turmeric that possesses a large number of medicinal properties. Recent studies show that curcumin possesses anticancer properties,[13,14] besides its many other uses as antioxidant,[15] anti-inflammatory,[16] and in treatment of cystic fibrosis[17] and Alzheimer's disease.[18] It can also act as a potential photodynamic therapy agent in skin cancer treatment, which has been demonstrated in a number of studies.[19,20]

The lack of bioavailability and extremely low stability in aqueous medium are the two major challenges faced in the application of curcumin as an effective agent for treating diseases. Curcumin has very poor aqueous solubility and tends to form aggregates and precipitate out in water, thus limiting its bioavailability.[21,22] It is also quite unstable in alkaline solutions and undergoes a pH-dependent degradation to form products like *trans*-6-(4′-hydroxy-3′-methoxyphenyl)-2,4-dioxo-5-hexenal, vanillin, and ferulic acid.[23,24] Wang et al. showed that addition of 10% calf serum can drastically slow down the degradation process,[23] which could be attributed to interactions between curcumin and serum components like serum albumin.[25] Interactions with surfactant aggregates, such as micelles, provide another important way to reduce curcumin

Received: June 16, 2014
Revised: August 22, 2014
Published: August 22, 2014

   dx.doi.org/10.1021/la5023533 | *Langmuir* 2014, 30, 10834−10844

Scheme 1. Different Forms of Curcumin

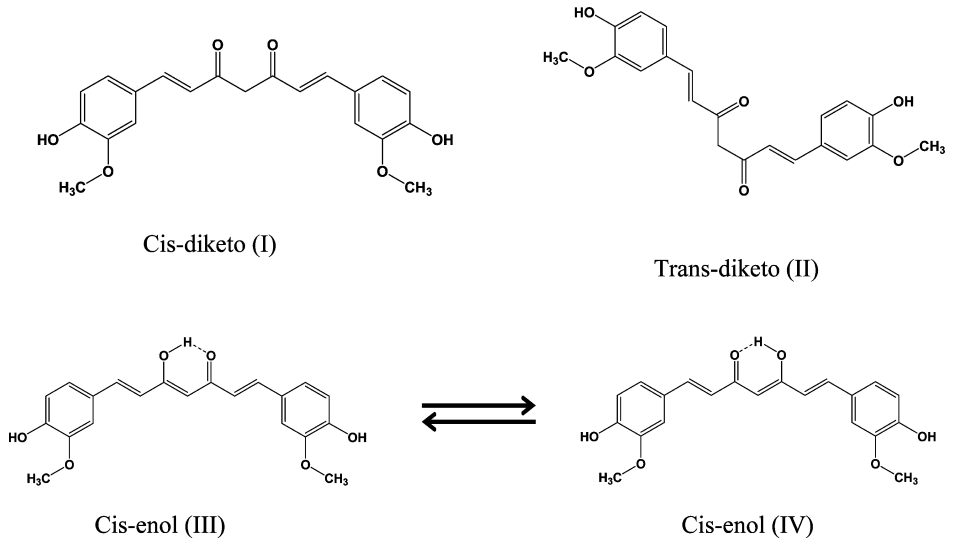

degradation.[26] Interestingly, in spite of a strong partitioning in lipidlike environments, oral administration to rats causes poor absorption through the gut with 38−75% being excreted in their feces.[27,28] Hence, studies for evaluation of the interactions of curcumin with membrane interfaces can be highly beneficial for controlling its degradation in water, which provide insight into in vivo interactions of the drug with the intestinal tract endothelial cell walls.

Structurally, curcumin is a β-diketone and exists in enol and keto tautomeric forms, as shown in Scheme 1. Due to the strong intramolecular hydrogen bond (H-bond) in the enol form, the β-diketone system undergoes transformation into a totally delocalized π-system.[29] The strengthening of the intramolecular hydrogen bond is strongly correlated to the π-system delocalization, which is supported by theoretical studies.[30,31] Moreover, when present in a solution, curcumin can even form intermolecular H-bonds with the solvent molecules which strongly influences its physicochemical properties in both the ground and excited states.[32] The interactions between curcumin and different carrier systems can be easily followed by monitoring the characteristic peaks of curcumin in the absorption as well as the fluorescence spectra. Thus, such spectroscopic methods have been utilized to gain insight into the transport and migration of bound curcumin in various biological systems.[33]

The monitoring of the excited state dynamics of a drug molecule is a renewed interest.[34−36] Some latest studies on curcumin in various media like neat solvents,[37−39] micelles,[40] and vesicles[41] elucidate the fact that one of the major photophysical processes in curcumin is the intramolecular hydrogen atom transfer between the hydroxyl group and the keto group of curcumin in the excited state followed by radiationless decay of excited-tautomer upon photoexcitation. The excited state dynamics of curcumin in various binary solvent mixtures has been reported recently by Das and Saini.[42,43] They showed that various properties such as polarity, viscosity, and hydrogen bonding played a vital role in the excited state dynamics of the pigment in toluene−alcohol mixture. The effects of acid and base have been extensively studied by Huppert and coworkers using time-resolved techniques.[44−46]

Considering the above factors, in this work, we have investigated the photophysical characteristics of curcumin inside different polymeric NPs at various temperatures. Three different polymers have been synthesized by reversible addition−fragmentation transfer (RAFT) technique. The curcumin encapsulated polymeric NPs were prepared by a simple sonication method. The encapsulation of curcumin was first studied using steady-state absorption and fluorescence spectroscopy, followed by fluorescence anisotropy measurements, and then to further exploit its photophysics time-resolved techniques were also applied at room temperature (298 K). The dependencies of the spectroscopic properties of the selected molecule curcumin inside the polymeric NPs with variation of temperature were also investigated.

2. EXPERIMENTAL SECTION

2.1. Materials. Curcumin was bought from Sigma-Aldrich with a purity of ∼81%. We have compared the absorption and fluorescence spectra of the purchased curcumin with the reported spectra of ∼99% pure curcumin and have found them to be similar. Thus, we could infer that 19% mass of the unknown compound present in our purchased curcumin has negligible effect on the spectral properties of curcumin. Milli-Q water was used throughout our experiments.

2.2. Instruments and Method. Dynamic light scattering (DLS) measurements were done using a Malvern Nano ZS instrument (model no. ZEN3600) having a thermostated sample chamber. All the measurements were carried out using a 4 mW He−Ne laser (λ = 632.8 nm) at a scattering angle of 173°. Field emission scanning electron microscope (FESEM) pictures were collected using a FEI NOVA NANOSEM 450 instrument working at 30 keV, and transmission electron microscope (TEM) pictures were taken using a (JEOL) JEM-2100 model operating at 200 keV. Samples for TEM were prepared by using a drop of polymeric NPs dispersed in water to blot a carbon-coated (50 nm carbon film) Cu grid (300 mesh, Electron Microscopy Science) and then allowing it to dry. Histograms were constructed manually by measuring the individual particle diameter uing Image-J software. A Shimadzu (model no. UV-2450) spectrophotometer was used to measure the absorption spectra, and a Hitachi (model no. F-7000) spectrofluorimeter was used for the measurement of the fluorescence spectra. Steady-state anisotropy measurement was done using a Horiba Jobin Yvon spectrofluorimeter (Fluoromax 4) with a 1 cm quartz cell. Steady state anisotropy can be defined as[47]

$$r_0 = \frac{I_{VV} - GI_{VH}}{I_{VV} + 2GI_{VH}} \quad (1)$$

dx.doi.org/10.1021/la5023533 | Langmuir 2014, 30, 10834−10844

Scheme 2. Synthesis Routes of Different Polymers by RAFT Reagents

(a) Synthesis of P1 polymer

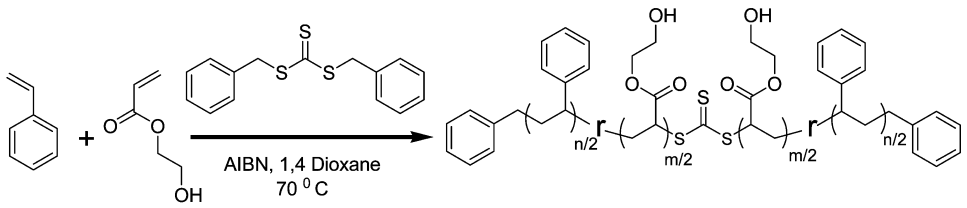

(b) Synthesis of P2 polymer

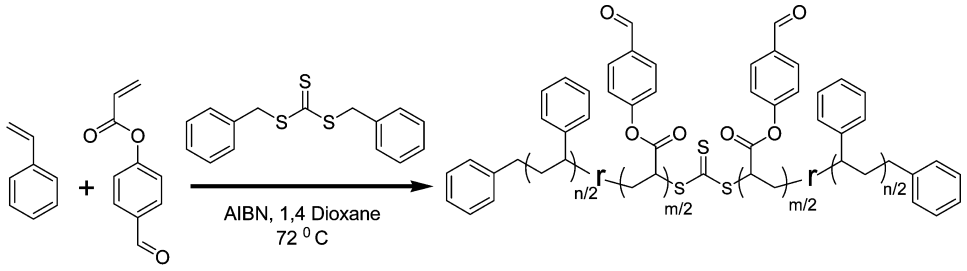

(c) Synthesis of P3 polymer

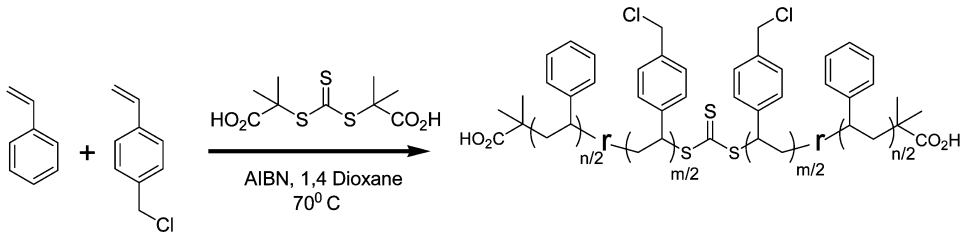

where G is the correction factor. I_{VV} and I_{VH} are the emission intensities of the sample with the when both the excitation and emission polarizer are oriented vertically, and when the excitation polarizer is oriented vertically but the emission polarizer is oriented horizontally, respectively. The fluorescence lifetime measurements were performed using a time-correlated single photon counting (TCSPC) spectrometer from IBH (U.K.). The details of the experimental setup have been provided in our earlier publication.[47] The signal, after excitation of the sample with a laser diode, was collected at a magic angle of 54.7° using a Hamamatsu microchannel plate photomultiplier tube (3809U). The fluorescence decays were monitored to the corresponding emission maxima obtained from steady state fluorescence measurement. The instrument response function (IRF) of our setup was ~90 ps. The data analysis was done using IBH DAS, version 6, decay analysis software, which was also used to analyze the anisotropy data. All the fluorescence decays were fitted with a biexponential function considering a χ^2 value close to 1, which is an indication of a good fit.

The average lifetimes of curcumin, after fitting the fluorescence transients with a biexponential function, were calculated using eq 2.[47]

$$\tau_{av} = a_1\tau_1 + a_2\tau_2 \quad (2)$$

where τ_1 and τ_2 are the first and second lifetime components, respectively, which were monitored at the emission maxima of the fluorophore, and a_1 and a_2 are the respective amplitudes of those components.

Considering the reported quantum yield (Φ) of C153 in acetonitrile, which is 0.56,[47,48] the Φ of curcumin was calculated.

2.3. Synthesis of Copolymers. The detailed synthetic procedure of the random copolymers has been described in the Supporting Information. Briefly, two different chain transfer agents (CTAs) (CTA1 and CTA2, Scheme 1) have been synthesized following the procedure described in the literature.[49,50] Poly(styrene-*ran*-2-hydroxyethyl acrylate) (P1) and poly(styrene-*ran*-4-formylphenyl acrylate) (P2) were synthesized by reacting styrene with 2-hydroxyethyl acrylate and 4-formylphenyl acrylate, respectively, in the presence of CTA2. Similarly, poly(styrene-*ran*-4-vinylbenzyl chloride) (P3) was synthesized by the reaction of styrene with 4-vinylbenzyl chloride in the presence of CTA1. The synthetic routes have been presented schematically in Scheme 2. The characterization data of the copolymers have been provided in the Supporting Information (Table S1).

2.4. Cytotoxicity Study. To evaluate the cell viability of synthesized polymers, $^3T_3$ fibroblast cells (source NCCS Pune) in DMEM (Himedia) with 10% FBS, 1% antibiotic, and 5% CO_2, at 10 000 cells/well were cultured and treated with various concentrations of the polymers followed by cytotoxicity detection using MTT assay. The percentages of viable fibroblast cells relative to the untreated control cells were more than 100% when cultured for 3 days with 40, 60, and 100 μL dispersion of all the polymers in water (10 mg/mL, Supporting Information Figure S4). The results indicate that all three polymers are biocompatible, among which the polymer P3 is the best.

2.5. Preparation of Polymeric NPs. Polymeric NPs of different sizes but having the same dye concentration, that can remain stable for more than a week, were synthesized following the procedure described elsewhere with slight modification.[51] First, a stock solution of curcumin in methanol was prepared, and the required amount of

dx.doi.org/10.1021/la5023533 | *Langmuir* 2014, 30, 10834−10844

the solution was taken in a vial and evaporated to dryness. Then, an appropriate volume of THF (100 μL) was added to maintain the concentration of curcumin at 0.3 mM. Next, different amounts of P1, P2, and P3 were taken in 200 μL of THF in separate vials, and finally, the polymeric solutions were introduced into round bottle flasks containing 2 mL of Milli-Q water with moderate stirring. After 15 s, the stock solution of curcumin was also introduced to the flask in dropwise manner. Then, the solutions of the three different polymers were stirred for about 15 min followed by vacuum evaporation of THF. Finally curcumin loaded polymeric NPs were obtained after 2 min of probe sonication of the above solutions. The mass of each of the polymers was taken in such a way that the final concentration of the polymer was 9×10^{-5} M and the final concentration of curcumin was 1.3×10^{-5} M. Membrane dialysis was used, having a molecular cut off of 3.5 KD, to determine the curcumin encapsulation efficiency. All the NPs showed good encapsulation efficiencies: for P1 and P2, it was nearly 80%; for P3, it was 68%.

2.6. Characterization of Curcumin Loaded Polymeric NPs. The characterizations of the dye loaded polymeric nanoparticles were performed by the help of DLS, FESEM, and TEM analysis. After the preparation of curcumin loaded polymeric NPs, DLS measurements were done to have an understanding of the structural features and stability of the same. As shown by the DLS histogram (Figure 1), the

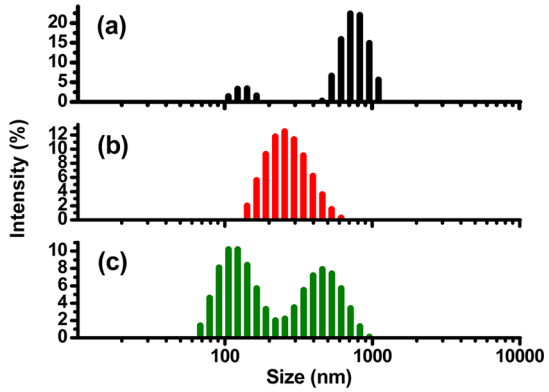

Figure 1. DLS size distribution plot of different polymeric NPs: (a) P1, (b) P2, and (c) P3.

hydrodynamic radius of the dye loaded polymeric NPs were different for the three polymers used in the present work. The NPs consisting of P1 showed a hydrodynamic diameter of 650 nm; for P2, the size of the NP was around 230 nm; while for the polymeric NP consisting of P3, two types of size distributions were observed. The sizes of the P3 NPs were 130 and 480 nm. Although DLS studies gave us an idea about the sizes of the synthesized polymeric NPs, their shape and morphology could not be confirmed. The shape of polymeric nanoparticles and their structural properties are much important factors determining their biocompatibility, which strongly depends on their interactions with various biomolecules like proteins and also different cells and tissues. Hence, it was essential to analyze the NPs using FESEM and TEM micrographs by directly measuring the particle diameter and constructing the particle size distribution histogram. The FESEM and TEM pictures are shown in Figure 2. The results obtained via FESEM and TEM were in accordance with the results obtained from DLS. Figure 2a and b clearly shows the spherical particles with the sizes comparable to DLS results for P1 and P2 NPs; Figure 2c also supports the DLS findings, with two types of spherical particles for P3 system. Figure 2d shows the TEM picture of the synthesized curcumin loaded polymeric NP composed of P2.

3. RESULTS AND DISCUSSION

3.1. Steady-State Absorption and Emission Studies. The absorption and emission spectra of curcumin inside different polymeric NPs were recorded. The absorption peaks

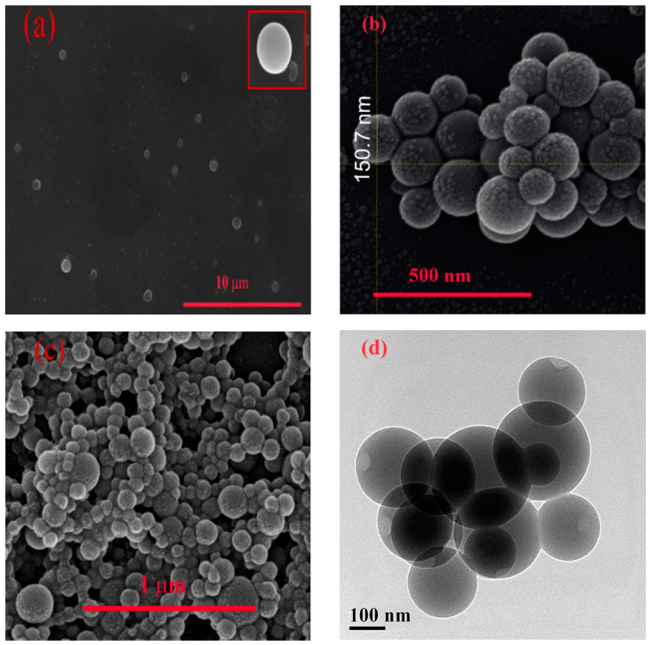

Figure 2. FESEM images of (a) P1, (b) P2, and (c) P3 polymeric NPs; (d) is the TEM image of P2 polymeric NPs.

of curcumin in water were obtained at 430 nm/355 nm. However, inside the polymeric NPs, the spectral nature and the peak positions changed depending on the nature of the polymeric NPs. The absorbance spectrum of curcumin in water is shown in Supporting Information Figure S5. The absorption band near 430 nm can be assigned to the lowest $\pi-\pi^*$ transitions occurring in curcumin, whereas the shoulder peak at 355 nm is assigned to the feruloyl unit's $\pi-\pi^*$ transitions.[52,53] As shown in Figure 3a, curcumin present inside P1 NPs showed the absorption peak at 427 nm with a shoulder near 452 nm, whereas that inside the P2 NPs showed absorption at 428 nm and a shoulder at 456 nm. Similarly, inside P3 NPs, it showed an absorption peak at 422 with a hump at 450 nm. As the solubility of curcumin in water is very low, it is necessary to measure its absorption spectra in a preferable solvent and compare the results. For that reason, we have taken the absorption spectra of curcumin in octanol (Supporting Information Figure S6). In octanol, curcumin showed a single absorption peak at around 429 nm. It was observed that the peak at around 350 nm vanished in both octanol as well as inside the NPs, suggesting a similarity between their environments. This observation was further supported by fluorescence results. The changes in the absorption spectrum of curcumin inside the polymeric NPs compared to that in bulk water indicated that the environment experienced by the probe molecules inside the polymeric NPs is different from that of water. These results suggested that curcumin behaves similarly within polymer NPs P1 and P2, but behave differently in P3 polymeric NPs. The different behaviors inside the different polymeric NPs could be due the difference in the type of interaction between curcumin and the NP. Curcumin possesses hydrophobic aryl groups as well as hydrophilic β-diketone groups, that possibly results in both van der Waals and electrostatic interactions with the polymeric NPs. Similar interactions of curcumin with cationic, anionic, zwitterionic, and neutral micelles have been reported in the literature, although the extent of interaction differed significantly

dx.doi.org/10.1021/la5023533 | Langmuir 2014, 30, 10834−10844

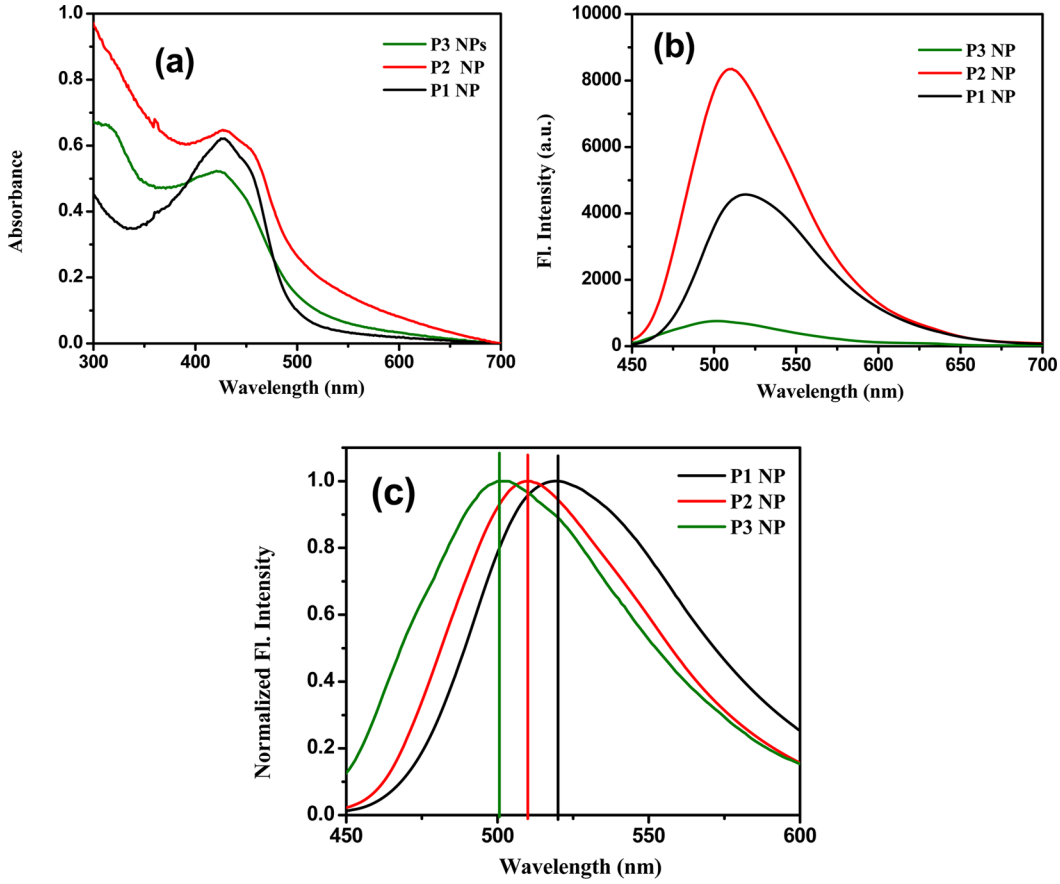

Figure 3. (a) Absorption and (b) emission spectra of curcumin in different polymeric NPs; (c) normalized emission spectra of curcumin in different polymeric NPs.

depending on the nature of interaction, that is, hydrophobic or electrostatic.[53,54]

In aqueous solution, curcumin shows a broad emission spectrum with low fluorescence intensity (Supporting Information Figure S5). The emission spectra of curcumin inside different polymeric NPs are shown in Figure 3b, and the normalized spectra are shown in Figure 3c. Inside the polymeric NPs, the fluorescence intensity as well as quantum yield was drastically increased, with a blue shift of nearly 30−50 nm. This type of huge blue shift in the emission spectrum of curcumin has been reported inside various micellar environments.[53,54] The presence of an emission peak at around 505 nm in octanol also suggests the presence of a hydrophobic environment sensed by curcumin inside polymeric NPs. However, it is also true that hydrophibicity is not the only reason to increase blue-shifted emission intensity as well as quantum yield. In the present study, the extent of blue shift depends on the functional group of the polymer molecules. The highest blue shift was observed for P3 NP where curcumin showed an emission peak at around 502 nm. Inside P1 NPs, curcumin showed a minimum blue shift with an emission maximum at 519 nm, while inside the P2 NPs it showed an intermediate blue shift with an emission maximum at around 510 nm. Upon close inspection of the above results, it was clear that the difference in emission maximum of curcumin inside different polymeric NPs is due to the difference in functional groups of the polymers. If we compare the structures of the polymers, it is easy to understand that the maximum blue shift of curcumin inside P3 NPs was due to the highest hydrophobicity provided by P3 compared to the others. We also determined the hydrophobicity (log *P*) of curcumin, which was 2.5, following the procedure described by Pal and Bhandari.[55] However, it should be noted that the polar groups at the end and middle should weaken the hydrophobic feature, and the fact that the overall log *P* value is 2.45 for curcumin is an indication of a highly hydrophobic bridge of curcumin. Hence, due to the presence of hydroxyethyl groups in P1 NPs, curcumin sensed a relatively polar environment that resulted in minimum blue shift. In P2 NPs, owing to the presence of formylphenyl groups, an intermediate polarity (compared to the other two polymeric NPs, P1 and P3) was felt by curcumin, resulting in intermediate value of the blue shift. All the absorption and emission peaks and Stokes shift are summarized in Supporting Information Table S2.

3.2. Determination of Steady State Anisotropy (r_0). The observations discussed earlier clearly indicated the existence of interaction between curcumin and the different polymeric NPs. Thus, in order to understand the pertinent as well as important issue of assessing the location of the probe inside the NPs, we have investigated the steady state anisotropy of curcumin inside the polymeric NPs. Deducing the precise location of the extrinsic molecular probe was indeed quite difficult. The rigidity of the microenvironment can be determined by the steady-state anisotropy measurement of our investigated dye molecule, which can provide information about any association or binding phenomenon occurring in the system. Therefore, from the measurement of the anisotropy value inside various polymeric NPs, one can gather valuable

dx.doi.org/10.1021/la5023533 | *Langmuir* 2014, 30, 10834−10844

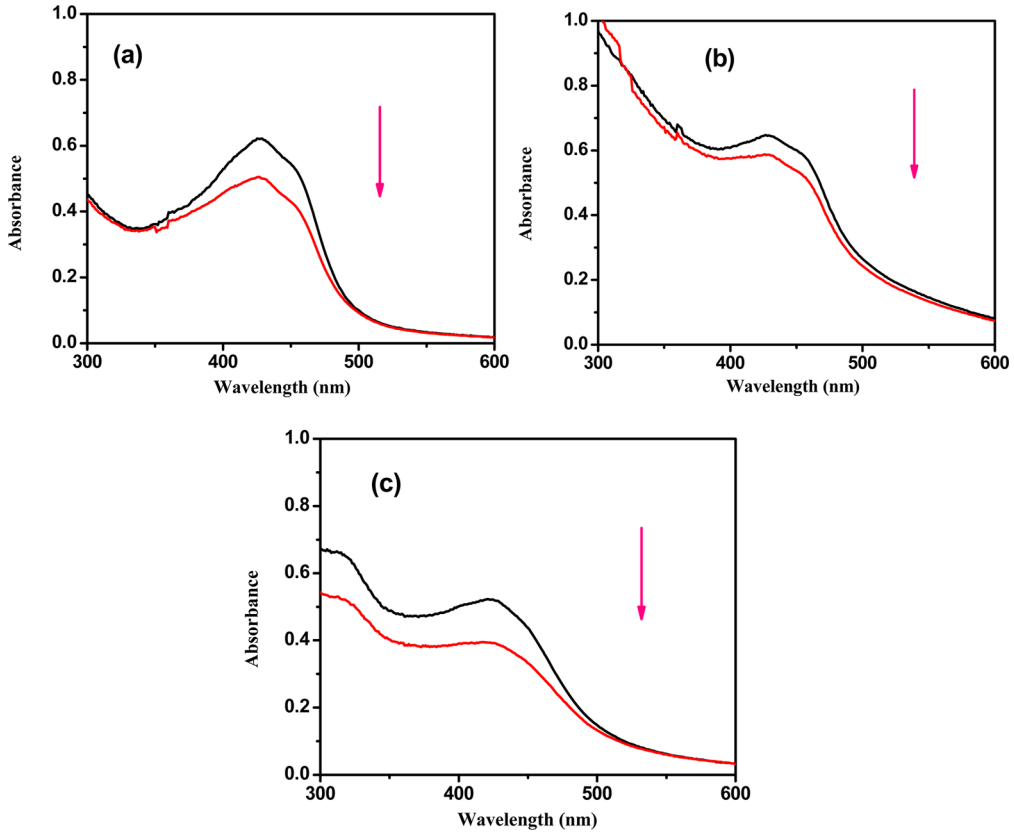

Figure 4. Changes in the absorption spectra of curcumin in different polymeric NPs with increasing time: (a) P1, (b) P2, and (c) P3 polymeric NPs.

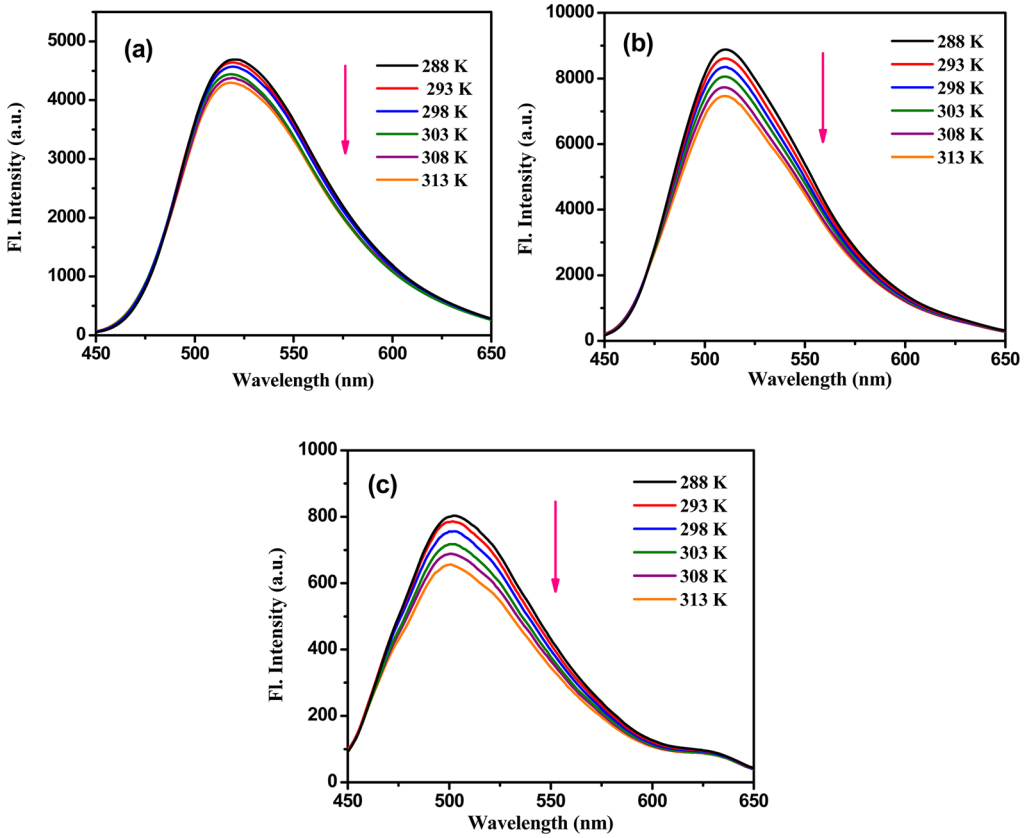

Figure 5. Emission spectra of curcumin in different polymeric NPs with variation of temperature: (a) P1, (b) P2, and (c) P3 polymeric NPs.

dx.doi.org/10.1021/la5023533 | *Langmuir* 2014, 30, 10834−10844

data about the microenvironment around the investigated drug molecule.[56,57] We measured the steady state fluorescence anisotropies (r_0) of curcumin inside the P1, P2, and P3 NPs. The obtained anisotropy values were quite interesting; they varied from one polymer NP to another. The anisotropy values are listed in Supporting Information Table S2. As we have already mentioned earlier, P3 NPs had the highest ability to provide a hydrophobic environment; hence, the highest anisotropy value of curcumin (0.1572) was obtained inside P3 NPs. This value is comparable to the value obtained in reverse micelle.[57] The anisotropy value of curcumin inside the other two polymeric NPs were 0.039 inside P1 and 0.047 inside P2. The low value of anisotropy was due to the presence of polar groups attached to the polymeric chains. Thus, it can be stated that curcumin feels more restriction inside P3 NPs owing to a more hydrophobic environment compared to the other two polymeric NPs.

3.3. Degradation Study. In this Article, we have also investigated the stabilities of curcumin inside all three polymeric NPs. Due to the presence of the unstable β-diketone linkage, curcumin dissociates into vanillin, ferulic acid, and feruloyl methane.[58] The degradation rate of curcumin had been monitored by taking the UV−vis spectra after certain intervals. It was reported that, after 1 h interval, 80% of curcumin was degraded in an aqueous buffer solution of pH 7.4.[58] In the present work, the extent of curcumin degradation inside the polymeric NPs was determined by monitoring the time-dependent absorption spectra, as shown in Figure 4. The degradation rate was found to be different inside different polymeric NPs. Inside P1 NPs, the degradation rate was 12%, for P2 NPs it was 7%, and for P3 NP the rate was nearly 19% after 48 h. Our results revealed that the polymeric NPs could act as a good stabilizer for curcumin. The different degradation rates inside different polymeric NPs could be explained by considering the interaction between curcumin and the functional groups of the respective polymers. Inside P3 NPs, the degradation rate was maximum; since there were no keto or enol groups present in P3, it was unable to form hydrogen bonds with the β-diketone linker of curcumin, leading to higher degradation rate.[53] Similar stability of curcumin inside P1 and P2 NPs was higher due to the presence of enol groups in P1 and keto groups in P2, both of which have the ability to form hydrogen bonds with the β-diketone linker of curcumin. Similar kinds of degradation rate were reported for curcumin on binding with hydrophobic cavities present in cyclodextrins and proteins.[58,59] Qian et al. recently established that the stability of curcumin increased drastically upon encapsulation into polymeric micelles.[60] Moreover, it was also demonstrated that the efficiency of intravenous application of curcumin loaded micelles is higher than that of free curcumin. From this point of view, polymeric NPs can be potentially good carriers of curcumin.

3.4. Effect of Temperature. The fluorescence intensity of curcumin decreased sharply with increase in temperature, as shown in Figure 5. On measuring the fluorescence intensity with variation in temperature, one can easily get an apparent idea regarding the binding ability of the probe with the polymeric NPs. We measured the fluorescence spectra of curcumin inside different polymeric NPs at various temperatures. Decrease in the fluorescence intensity of curcumin with increase in temperature could be due to the enhancement of nonradiative transition as well as the decrease in interaction between curcumin and polymeric NPs at elevated temperature. Now, to compare the thermal stability of curcumin inside different polymeric NPs, we plotted the fluorescence intensity of curcumin as a function of temperature by normalizing with the highest fluorescence intensity (Figure 6). From the slope of

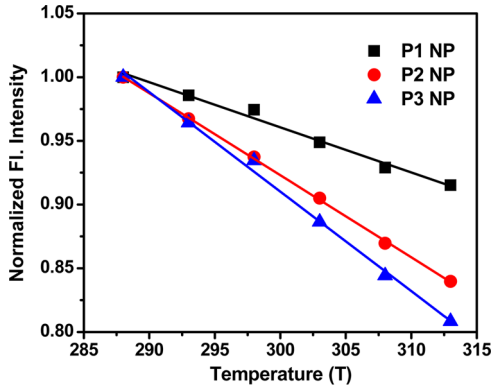

Figure 6. Changes in the fluorescence intensity of curcumin with variation of temperature inside different polymeric NPs with increasing temperature: (black squares) P1, (red circles) P2, and (blue triangles) P3 polymeric NPs.

Figure 6, we may conclude that the P1 and P2 NPs were better stabilizers for curcumin at elevated temperature compared to P3 NPs. The highest slope of fluorescence intensity vs temperature plot in the case of P3 NPs indicates the least stability of curcumin inside P3 NPs.

3.5. Time-Resolved Studies. The fluorescence decays of the probe, curcumin, inside different polymeric NPs were recorded with an excitation wavelength of 408 nm, and the fluorescence decays were monitored to its emission maxima inside different polymeric NPs. Figure 7 represents the fluorescence decay profiles of curcumin inside different polymeric NPs. The lifetime values were obtained by fitting the fluorescence decay curves biexponentially, as tabulated in Table 1. Fluorescence lifetime, being highly sensitive to the environment and also the excited state interactions, serves as an indicator to study and understand the environment surrounding a fluorophore.[61,62] Here, we have recorded and monitored the fluorescence lifetime of curcumin to interpret the location of the probe molecule in the heterogeneous media. The fluorescence lifetime of the probe molecule varies for different microheterogeneous systems like micelles, reverse micelles, and vesicles. In most of the cases, the fluorescence decay profiles show a multiexponential fitting.[63] In the present study, the fluorescence decay of curcumin was found to be biexponential having χ^2 values near to 1 (Table 1), which suggested the local heterogeneity in the distribution of the probe, although its location was considered to be mostly inside the polymeric NPs. The different modes of interaction between curcumin and various functional groups of polymers are the reasons behind the heterogeneity. Having the complex mode of interaction, it is simpler to account for the average fluorescence lifetime of the probe molecules instead of emphasizing both components. Equation 2 was applied to calculate the average fluorescence lifetime of curcumin.

The components of fluorescence decays of curcumin were attributed mainly because of two processes, excited state intramolecular proton transfer (ESIPT)[33] and solvation.[63] Curcumin forms a six-membered chelate ring in nonpolar solvent, which facilitates the ESIPT process responsible to show

dx.doi.org/10.1021/la5023533 | Langmuir 2014, 30, 10834−10844

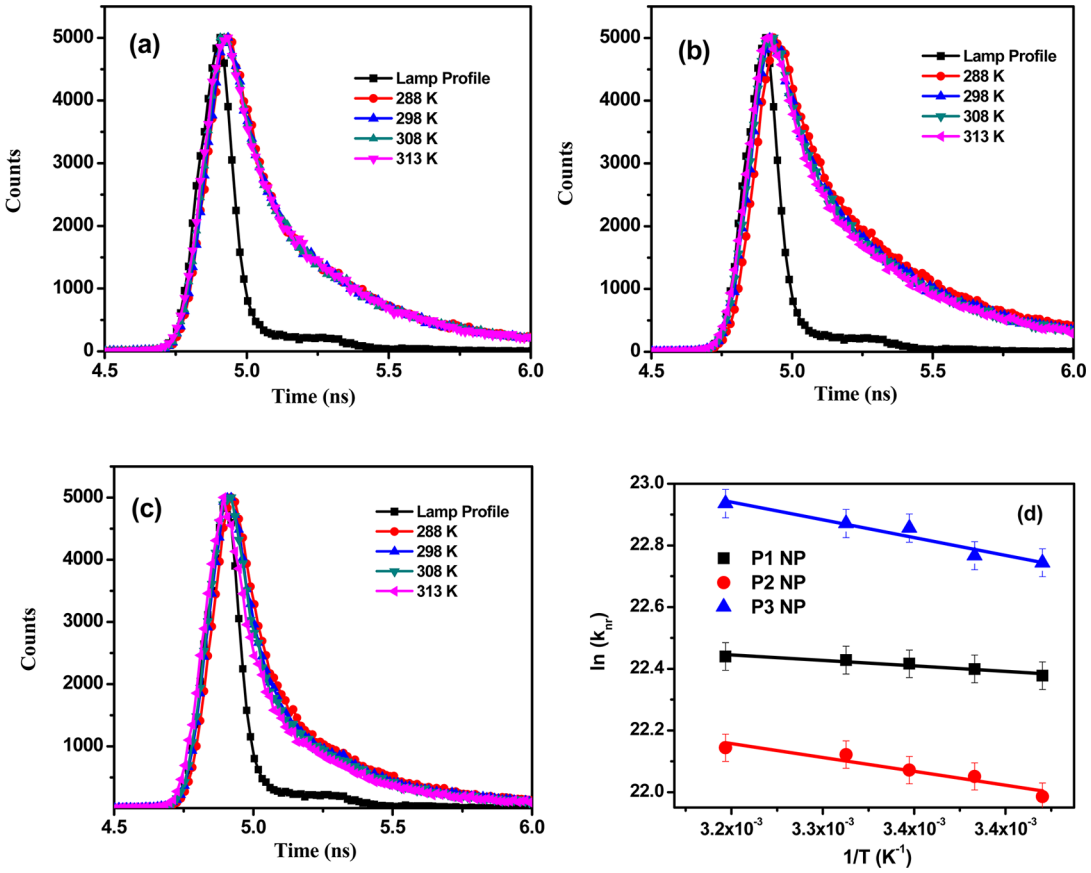

Figure 7. Time resolved lifetime decays of curcumin in different polymeric NPs with increasing temperature: (a) P1, (b) P2, and (c) P3 polymeric NPs. (d) Arrhenius plot for different polymeric NPs.

Table 1. Fluorescence Lifetime, Quantum Yield, Nonradiative Rate, and Radiative Rate Constants of Curcumin in P1, P2, and P3 Polymeric NPs with Variation of Temperature

	τ_1 (a_1) (ns)	τ_2 (a_2) (ns)	$\langle\tau\rangle$ (ns)[a]	quantum yield (Φ_X)	K_{nr} (s^{-1})/10^9	K_r (s^{-1})/10^8
curcumin in P1 polymeric NPs						
288 K	0.130(0.88)	0.605(0.12)	0.187	0.0219	5.230	1.171
293 K	0.125(0.86)	0.541(0.14)	0.183	0.0217	5.346	1.186
298 K	0.124(0.86)	0.526(0.14)	0.180	0.0214	5.437	1.189
303 K	0.117(0.85)	0.526(0.15)	0.178	0.0207	5.502	1.163
313 K	0.113(0.83)	0.489(0.17)	0.176	0.0203	5.566	1.153
curcumin in P2 polymeric NPs						
288 K	0.176(0.82)	0.716(0.18)	0.273	0.0354	3.533	1.297
293 K	0.162(0.82)	0.687(0.18)	0.256	0.0344	3.772	1.344
298 K	0.156(0.81)	0.658(0.19)	0.251	0.0333	3.851	1.327
303 K	0.145(0.80)	0.615(0.20)	0.239	0.0323	4.049	1.351
313 K	0.141(0.80)	0.607(0.20)	0.234	0.0311	4.140	1.329
curcumin in P3 polymeric NPs						
288 K	0.098(0.92)	0.523(0.08)	0.132	0.0045	7.542	0.3409
293 K	0.094(0.91)	0.490(0.09)	0.129	0.0044	7.718	0.3411
298 K	0.083(0.90)	0.436(0.10)	0.118	0.0042	8.439	0.3559
303 K	0.082(0.90)	0.424(0.10)	0.116	0.0040	8.568	0.3448
313 K	0.074(0.89)	0.393(0.11)	0.109	0.0039	9.138	0.3578

[a]Error in experimental data ± 10%

a very short lifetime of a few hundred femtoseconds. However, in polar solvent, due to the disruption of the ESIPT process, the lifetime of curcumin shows a value of 130 ps.[64] The similarity observed between the time constant of ESIPT and the fluorescence lifetime in our systems established the fact that ESIPT was the principal photophysical process of curcumin in the excited state. The lifetime values of curcumin inside different polymeric NPs were found to be different as shown in Table 1. For P1 NPs, the lifetime value of curcumin was 180 ps with components 124 ps (86%) and 526 ps (14%). The average lifetime value inside P2 NPs was 251 ps with components 156 ps (81%) and 658 ps (19%). The lowest average lifetime value

dx.doi.org/10.1021/la5023533 | Langmuir 2014, 30, 10834−10844

was obtained inside P3 NPs, where it showed the average lifetime value of 118 ps with components 83 ps (90%) and 436 ps (10%) at 298 K. The variation in lifetime values of curcumin in different polymeric NPs can be explained by considering the ESIPT process, the main photophysics operating on the excited state of curcumin. As we have already mentioned in the steady state section that due to the presence of enol group in P1 NP and keto group in the P2 NP, both P1 and P2 can perturb the ESIPT process of curcumin in the excited state of curcumin, leading to higher lifetime values. Similar findings were obtained in our earlier studies, where we showed that the ESIPT process of curcumin is perturbed inside reverse micelles as well as other organized media.[57] In water, curcumin shows the lifetime value of nearly 30 ps. However, inside P3 NP, the lifetime value was quite high, which suggested that the van der Waals interactions that exist between the two phenyl moieties of curcumin and the hydrophobic chain of the polymer can also increase the lifetime values, although the ESIPT process has the larger effect on lifetime value of curcumin compared to van der Waals interaction.

In order to further realize the effect of encapsulation of curcumin on the overall radiative (k_r) and nonradiative (k_{nr}) decay rates, the following equations were used:

$$k_r = \frac{\phi_f}{\langle \tau \rangle_f} \tag{3}$$

$$k_{nr} = \frac{1}{\langle \tau \rangle_f} - k_r \tag{4}$$

The calculated values are provided in Table 1. The change in the radiative decay rate is negligible compared to the nonradiative rate for all the cases mentioned above. From Table 1, it is clear that inside the P1 NPs the nonradiative rate constant of curcumin was 5.437×10^9 S^{-1} and inside the P2 NPs it was 3.851×10^9 S^{-1}. However, inside P3 NPs, it showed a quite high nonradiative rate constant, which was 8.439×10^9 S^{-1} at 298 K. The high value of nonradiative rate constant inside P3 NPs also supported our previous assumption that the van der Waals interactions operating on curcumin inside P3 NPs was not sufficient enough to reduce the nonradiative rate constant of curcumin. Disturbance of ESIPT process inside the P1 and P2 NPs was the reason to get lower nonradiative rate constant. As per the consideration that the ESIPT (excited state intramolecular proton transfer) process in curcumin is a nonradiative process, the major changes in the nonradiative rates revealed the fact that intermolecular hydrogen bonding in the excited state, occurring between curcumin and P1, P2 NPs, led to a significant perturbation of the excited state dynamics of curcumin.

Temperature dependent lifetime measurements have also been performed, as tabulated in Table 1, with the representative fluorescence transients that are shown in Figure 7. With increase in temperature from 288 to 313 K, the rate constant for nonradiative process of curcumin increased from 5.230×10^9 to 5.566×10^9 S^{-1} inside P1 NPs. The same value changed from 3.533×10^9 to 4.140×10^9 S^{-1} inside P2 NPs, while due to the lower thermal stability of curcumin inside P3 NPs the change in the nonradiative rate constant was high. Inside P3 NPs, it increased from 7.542×10^9 to 9.138×10^9 S^{-1}. The increase in nonradiative rate can be justified by considering the fact that, at higher temperature, the accessibility of water into the polymeric NPs increased as a result of which water-assisted nonradiative decay channels also increased. Temperature dependent experiments have been performed to calculate the activation energies of the nonradiative decay process of curcumin inside different polymeric NPs. Figure 7d shows the Arrhenius plot of $\ln(k_{nr})$ versus $1/T$. From the slope of the plot, the activation energies inside different polymeric NPs have been calculated. The activation energy values obtained from the plot were1.84, 4.67, and 5.99 kJ/mol for P1, P2, and P3 NPs, respectively. The calculated values inside the polymeric NPs were slightly less compared to that in micellar system.[53]

3.6. Release Study. After monitoring the ESIPT process of curcumin inside the polymeric NPs, steady state fluorescence spectroscopy was used to study whether the NPs are capable of releasing the entrapped curcumin or not. Surprisingly, it was observed that all the NPs have the ability to release curcumin at pH ∼ 3. The decrease in fluorescence intensity is an implication of the release of curcumin from the polymeric NPs. In other words, the huge decrease in intensity of the emission spectrum of curcumin with decrease in pH is an indication of the movement of curcumin from the polymeric NPs to bulk water. The steady state fluorescence results are shown in Supporting Information Figure S7. These results suggest that although the synthesized polymeric NPs are stable at neutral pH for several months, they are not stable at acidic pH (the stability of the NPs decreases with decrease in pH). At pH 3, the disruption of the nanocontainers leads to the release of curcumin. The instability of NPs in acidic pH can be used for pH-triggered release of hydrophobic drug molecules in the diseased cells.

3.7. Comparative Study. To comprehend the ESIPT process inside different polymeric NPs, it is essential to make a comparative statement. From the steady state study, it was observed that the extent of increase in fluorescence intensity of curcumin inside different polymeric NPs followed the order: P2 > P1 > P3. As the ESIPT process decreases the fluorescence intensity of curcumin, the highest fluorescence intensity inside P2 NPs proves its ability to reduce the ESIPT process more as compared to the other two NPs. This observation was further supported by time-resolved experiments. Inside P2 NPs, the lifetime value of curcumin was twice of that in P3 NPs. As a result, we can say that although all the NPs have the ability to modulate the ESIPT process, P2 NPs are the most efficient.

4. CONCLUSION

We have synthesized three different random copolymers possessing different functional groups that have been utilized to form polymeric NPs. It was observed that all the polymeric NPs were capable of incorporating curcumin. The rate of curcumin degradation was drastically suppressed inside all the polymeric NPs. The higher lifetime value of curcumin inside the polymeric NPs indicated the changes in the excited state dynamics of curcumin. Depending on the functional group of the polymeric NPs, the lifetime value of curcumin changed. The presence of keto or enol groups in polymeric NPs, like P1 and P2, are very much suitable to perturb the ESIPT process of curcumin. Temperature dependent lifetime measurements were also performed to demonstrate their thermal stability. The activation energies for nonradiative decay inside different polymeric NPs were also calculated. An extremely low hydrolytic degradation rate of curcumin encapsulated inside the polymeric NPs makes it an effective and smart nano-compartment for being a drug delivery vehicle.

dx.doi.org/10.1021/la5023533 | Langmuir 2014, 30, 10834−10844

■ ASSOCIATED CONTENT

Supporting Information

The detailed synthesis procedure of random copolymers, various steady state parameters and figures, MTT assay results. This material is available free of charge via the Internet at http://pubs.acs.org.

■ AUTHOR INFORMATION

Corresponding Authors

*E-mail: nilmoni@chem.iitkgp.ernet.in. Fax: 91-3222-255303.
*E-mail: dibakar@chem.iitkgp.ernet.in.

Notes

The authors declare no competing financial interest.

■ ACKNOWLEDGMENTS

N.S. is thankful to Council of Scientific and Industrial Research (CSIR) for a generous research grant. D.D. thanks SRIC, IIT Kharagpur for research grant (Project codes ADA and NPA with institute approval numbers - IIT/SRIC/CHY/ADA/2014-15/18 and IIT/SRIC/CHY/NPA/2014-15/81, respectively). C.B. and J.K. are thankful to UGC, S.M. is thankful to CSIR, and D.B. and N.K. are thankful to IIT Kharagpur for their research fellowships.

■ REFERENCES

(1) LaVan, D. A.; McGuire, T.; Langer, R. Small-scale systems for in vivo drug delivery. *Nat. Biotechnol.* **2003**, *21*, 1184−1191.
(2) Langer, R. New methods of drug delivery. *Science* **1990**, *249*, 1527−1533.
(3) Davis, M. E.; Chen, Z. G.; Shin, D. M. Nanoparticle therapeutics: An emerging treatment modality for cancer. *Nat. Rev. Drug Discovery* **2008**, *7*, 771−782.
(4) Farokhzad, O. C.; Langer, R. Nanomedicine: Developing smarter therapeutic and diagnostic modalities. *Adv. Drug Delivery Rev.* **2006**, *58*, 1456−1459.
(5) Peer, D.; Karp, J. M.; Hong, S.; Farokhzad, O. C.; Margalit, R.; Langer, R. Nanocarriers as an emerging platform for cancer therapy. *Nat. Nanotechnol.* **2007**, *2*, 751−760.
(6) Cuong, N. V.; Hsieh, M. F. Recent advances in pharmacokinetics of polymeric excipients used in nanosized anti-cancer drugs. *Curr. Drug Metab.* **2009**, *10*, 842−850.
(7) Tong, R.; Cheng, J. Anticancer polymeric nanomedicines. *Polym. Rev.* **2007**, *47*, 345−381.
(8) Bouladjine, A.; Al-Kattan, A.; Dufour, P.; Drouet, C. New advances in nanocrystalline apatite colloids intended for cellular drug delivery. *Langmuir* **2009**, *25*, 12256−12265.
(9) Wang, H.; Xu, J.; Wang, J.; Chen, T.; Wang, Y.; Tan, Y. W.; Su, H.; Chan, K. L.; Chen, H. Probing the kinetics of short-distance drug release from nanocarriers to nanoacceptors. *Angew. Chem.* **2010**, *49*, 8426−8430.
(10) Chen, H.; Kim, S.; Li, L.; Wang, S.; Park, K.; Cheng, J. X. Release of hydrophobic molecules from polymer micelles into cell membranes revealed by Forster resonance energy transfer imaging. *Proc. Natl. Acad. Sci. U.S.A.* **2008**, *105*, 6596−6601.
(11) Diezi, T. A.; Bae, Y.; Kwon, G. S. Enhanced stability of PEGblock- poly(*N*-hexyl stearate L-aspartamide) micelles in the presence of serum proteins. *Mol. Pharmaceutics* **2010**, *7*, 1355−1360.
(12) Kamaly, N.; Xiao, Z.; Valencia, P. M.; Radovic-Morenob, A. F.; Farokhzad, O. C. Targeted polymeric therapeutic nanoparticles: Design, development and clinical translation. *Chem. Soc. Rev.* **2012**, *41*, 2971−3010.
(13) Aggarwal, B. B.; Kumar, A.; Bharti, A. C. Anticancer potential of curcumin: Preclinical and clinical studies. *Anticancer Res.* **2003**, *23*, 363−398.
(14) Shi, M.; Cai, Q.; Yao, L.; Mao, Y.; Ming, Y.; Ouyang, G. Antiproliferation and apoptosis induced by curcumin in human ovarian cancer cells. *Cell Biol. Int.* **2006**, *30*, 221−226.
(15) Ruby, A. J.; Kuttan, G.; Babu, K. D.; Rajasekharan, K. N.; Kuttan, R. Anti-tumour and antioxidant activity of natural curcuminoids. *Cancer Lett.* **1995**, *94*, 79−83.
(16) Lantz, R. C.; Chen, G. J.; Solyom, A. M.; Jolad, S. D.; Timmermann, B. N. The effect of turmeric extracts on inflammatory mediator production. *Phytomedicine* **2005**, *12*, 445−452.
(17) Egan, M. E.; Pearson, M.; Weiner, S. A.; Rajendran, V.; Rubin, D.; Glockner-Pagel, J.; Canny, S.; Du, K.; Lukacs, G. L.; Caplan, M. J. Curcumin, a major constituent of turmeric, corrects cystic fibrosis defects. *Science* **2004**, *304*, 600−602.
(18) Yang, F.; Lim, G. P.; Begum, A. N.; Ubeda, O. J.; Simmons, M. R.; Ambegaokar, S. S.; Chen, P.; Kayed, R.; Glabe, C. G.; Frautschy, S. A.; Cole, G. M. Curcumin inhibits formation of amyloid beta oligomers and fibrils, binds plaques, and reduces amyloid in vivo. *J. Biol. Chem.* **2005**, *280*, 5892−5901.
(19) Koon, H.; Leung, A. W. N.; Yue, K. K. M.; Mak, N. K. Photodynamic effect of curcumin on NPC/CNE2 cells. *J. Environ. Pathol., Toxicol. Oncol.* **2006**, *25*, 205−215.
(20) Park, K.; Lee, J.-H. Photosensitizer effect of curcumin on UVB-irradiated HaCaT cells through activation of caspase pathways. *Oncol. Rep.* **2007**, *17*, 537−540.
(21) Leung, M. H. M.; Kee, T. W. Effective stabilization of curcumin by association to plasma proteins: Human serum albumin and fibrinogen. *Langmuir* **2009**, *25*, 5773−5777.
(22) Leung, M. H. M.; Colangelo, H.; Kee, T. W. Encapsulation of curcumin in cationic micelles suppresses alkaline hydrolysis. *Langmuir* **2008**, *24*, 5672−5675.
(23) Wang, Y. J.; Pan, M. H.; Cheng, A. L.; Lin, L. I.; Ho, Y. S.; Hsieh, C. Y.; Lin, J. K. Stability of curcumin in buffer solutions and characterization of its degradation products. *J. Pharm. Biomed. Anal.* **1997**, *15*, 1867−1876.
(24) Toennesen, H. H.; Karlsen, J. Studies on curcumin and curcuminoids. VI. Kinetics of curcumin degradation in aqueous solution. *Z. Lebensm.-Unters. -Forsch.* **1985**, *180*, 402−404.
(25) Patra, D.; Barakat, C.; Tafech, R. M. Study on effect of lipophilic curcumin on sub-domain IIA site of human serum albumin during unfolded and refolded states: A synchronous fluorescence spectroscopic study. *Colloids Surf., B* **2012**, *94*, 354−361.
(26) Boruaha, B.; Saikiab, P. M.; Duttaa, R. K. Binding and stabilization of curcumin by mixed chitosan−surfactant systems: A spectroscopic study. *J. Photochem. Photobiol., A* **2012**, *245*, 18−27.
(27) Ravindranath, V.; Chandrasekhara, N. Metabolism of curcumin—Studies with [3H] curcumin. *Toxicology* **1981**, *22*, 337−344.
(28) Wahlstrom, B.; Blennow, G. A study on the fate of curcumin in the rat. *Acta Pharmacol. Toxicol.* **1978**, *43*, 86−92.
(29) Gilli, G.; Bertolasi, V. In *The Chemistry of Enols*; Rappoport, Z., Ed.; John Wiley & Sons: New York, 1990; pp 713−764.
(30) Balasubramanian, K. Molecular orbital basis for yellow curry spice curcumin's prevention of Alzheimer's disease. *J. Agric. Food Chem.* **2006**, *54*, 3512−3520.
(31) Shen, L.; Ji, H. F.; Zhang, H. Y. A TD-DFT study on triplet excited-state properties of curcumin and its implications in elucidating the photosensitizing mechanisms of the pigment. *Chem. Phys. Lett.* **2005**, *409*, 300−303.
(32) Saini, R. K.; Das, K. Picosecond spectral relaxation of curcumin excited state in a binary solvent mixture of toluene and methanol. *J. Phys. Chem. B* **2012**, *116*, 10357−10363.
(33) Harada, T.; Giorgio, L.; Harris, T. J.; Pham, D.-T.; Ngo, H. T.; Need, E. F.; Coventry, B. J.; Lincoln, S. F.; Easton, C. J.; Buchanan, G.; Kee, T. W. Diamide linked γ-cyclodextrin dimers as molecular-scale delivery systems for the medicinal pigment curcumin to prostate cancer cells. *Mol. Pharmaceutics* **2013**, *10*, 4481−4490.
(34) Bonancía, P.; Vaya, I.; JoséCliment, M.; Gustavsson, T.; Markovitsi, D.; Jimenez, M. C.; Miranda, M. A. Excited-state

interactions in diastereomeric flurbiprofen−thymine dyads. *J. Phys. Chem. A* **2012**, *116*, 8807−8814.
(35) Miannay, F. A.; Gustavsson, T.; Banyasz, A.; Markovitsi, D. Excited-state dynamics of dGMP measured by steady-state and femtosecond fluorescence spectroscopy. *J. Phys. Chem. A* **2010**, *114*, 3256−3263.
(36) Akos Banyasz, A.; Douki, T.; Improta, R.; Gustavsson, T.; Onidas, D.; Vaya, I.; Perron, M.; Markovitsi, D. Electronic excited states responsible for dimer formation upon UV absorption directly by thymine strands: Joint experimental and theoretical study. *J. Am. Chem. Soc.* **2012**, *134*, 14834−14845.
(37) Jasim, F.; Ali, F. A novel and rapid method for the spectrofluorometric determination of curcumin in curcumin spices and flavors. *Microchem. J.* **1992**, *46*, 209−214.
(38) Began, G.; Sudharshan, E.; Udaya, S. K.; Appu Rao, A. G. Interaction of curcumin with phosphatidylcholine: A spectrofluorometric study. *J. Agric. Food Chem.* **1999**, *47*, 4992−4997.
(39) Khopde, S. M.; Priyadarsini, K. I.; Palit, D. K.; Mukherjee, T. Effect of solvent on the excited-state photophysical properties of curcumin. *Photochem. Photobiol.* **2000**, *72*, 625−631.
(40) Kapoor, S.; Priyadarsini, K. I. Protection of radiation-induced protein damage by curcumin. *Biophys. Chem.* **2001**, *92*, 119−126.
(41) Kunwar, A.; Barik, A.; Pandey, R.; Priyadarsini, K. I. Transport of liposomal and albumin loaded curcumin to living cells: An absorption and fluorescence spectroscopic study. *Biochim. Biophys. Acta* **2006**, *1760*, 1513−1520.
(42) Saini, R. K.; Das, K. Picosecond spectral relaxation of curcumin excited state in toluene−alcohol mixtures. *J. Lumin.* **2013**, *144*, 169−175.
(43) Saini, R. K.; Das, K. Photophysics of Curcumin excited state in toluene-polar solvent mixtures: Role of H-bonding properties of the polar solvent. *J. Lumin.* **2014**, *145*, 832−837.
(44) Erez, Y.; Simkovitch, R.; Shomer, S.; Gepshtein, R.; Huppert, D. Effect of acid on the ultraviolet−visible absorption and emission properties of curcumin. *J. Phys. Chem. A* **2014**, *118*, 872−884.
(45) Akulov, K.; Simkovitch, R.; Erez, Y.; Gepshtein, R.; Schwartz, T.; Huppert, D. Acid effect on photobase properties of curcumin. *J. Phys. Chem. A* **2014**, *118*, 2470−2479.
(46) Erez, Y.; Presiado, I.; Gepshtein, R.; Huppert, D. The effect of a mild base on curcumin in methanol and ethanol. *J. Phys. Chem. A* **2012**, *116*, 2039−2048.
(47) Hazra, P.; Chakrabarty, D.; Sarkar, N. Solvation dynamics of coumarin 153 in aqueous and non-aqueous reverse micelles. *Chem. Phys. Lett.* **2003**, *371*, 553−562.
(48) Jones, G. II; Jackson, W. R.; Choi, C.-Y.; Bergmark, W. R. Solvent effect on emission yield and lifetime of coumarin laser dyes: Requirements for rotatory decay mechanism. *J. Phys. Chem.* **1985**, *89*, 294−300.
(49) Lai, J. T.; Filla, D.; Shea, R. Functional polymers from novel carboxyl-terminated trithiocarbonates as highly efficient RAFT agents. *Macromolecules* **2002**, *35*, 6754−6756.
(50) Banerjee, R.; Dhara, D. Functional group-dependent self-assembled nanostructures from thermo-responsive triblock copolymers. *Langmuir* **2014**, *30*, 4137−4146.
(51) Bhattacharyya, S.; Sen, T.; Patra, A. Host−guest energy transfer: Semiconducting polymer nanoparticles and Au nanoparticles. *J. Phys. Chem. C* **2010**, *114*, 11787−11795.
(52) Ke, D.; Wang, X.; Yang, Q.; Niu, Y.; Chai, S.; Chen, Z.; An, X.; Shen, W. Spectrometric study on the interaction of dodecyltrimethylammonium bromide with curcumin. *Langmuir* **2011**, *27*, 14112−14117.
(53) Banerjee, C.; Ghosh, S.; Mandal, S.; Kuchlyan, J.; Kundu, N.; Sarkar, N. Exploring the photophysics of curcumin in zwitterionic micellar system: An approach to control ESIPT process in the presence of room temperature ionic liquids (RTILs) and anionic surfactant. *J. Phys. Chem. B* **2014**, *118*, 3669−3681.
(54) Adhikary, R.; Carlson, P. J.; Kee, T. W.; Petrich, J. W. Excited-state intramolecular hydrogen atom transfer of curcumin in surfactant micelles. *J. Phys. Chem. B* **2010**, *114*, 2997−3004.
(55) Bhandari, R.; Pal, K. I. A method to prepare solid lipid nanoparticles with improved entrapment efficiency of hydrophilic drugs. *Curr. Nanosci.* **2013**, *9*, 211−220.
(56) Mandal, S.; Banerjee, C.; Ghosh, S.; Kuchlyan, J.; Sarkar, N. Modulation of the photophysical properties of curcumin in non-ionic surfactant (Tween-20) forming micelles and niosomes: A comparative study of different microenvironments. *J. Phys. Chem. B* **2013**, *117*, 6957−6968.
(57) Banerjee, C.; Ghatak, C.; Mandal, S.; Ghosh, S.; Kuchlyan, J.; Sarkar, N. Curcumin in reverse micelle: An example to control excited-state intramolecular proton transfer (ESIPT) in confined media. *J. Phys. Chem. B* **2013**, *117*, 6906−6916.
(58) Harada, T.; Pham, D.-T.; Leung, M. H. M.; Ngo, H. T.; Lincoln, S. F.; Easton, C. J.; Kee, T. W. Cooperative binding and stabilization of the medicinal pigment curcumin by diamide linked γ-cyclodextrin dimers: A spectroscopic characterization. *J. Phys. Chem. B* **2011**, *115*, 1268−1274.
(59) Leung, M. H. M.; Kee, T. W. Effective stabilization of curcumin by association to plasma proteins: Human serum albumin and fibrinogen. *Langmuir* **2009**, *25*, 5773−5777.
(60) Gou, M.; Men, K.; Shi, S. H.; Xiang, L. M.; Zhang, J.; Song, J.; Long, L. J.; Wan, Y.; Luo, F.; Zhao, X.; Qian, Y. Z. Curcumin-loaded biodegradable polymeric micelles for colon cancer therapy in vitro and in vivo. *Nanoscale* **2011**, *3*, 1558−1567.
(61) Paul, B. K.; Samanta, A.; Guchhait, N. Modulation of excited-state intramolecular proton transfer reaction of 1-hydroxy-2-naphthaldehyde in different supramolecular assemblies. *Langmuir* **2010**, *26*, 3214−3224.
(62) Paul, B. K.; Guchhait, N. Modulated photophysics of an ESIPT probe 1-hydroxy-2-naphthaldehyde within motionally restricted environments of liposome membranes having varying surface charges. *J. Phys. Chem. B* **2010**, *114*, 12528−12540.
(63) Nardo, L.; Andreoni, A.; Masson, M.; Haukvik, T.; Tønnesen, H. H. Studies on curcumin and curcuminoids. XXXIX. Photophysical properties of bisdemethoxycurcumin. *J. Fluoresc.* **2011**, *21*, 627−635.
(64) Ghosh, R.; Mondal, J. A.; Palit, D. K. Ultrafast dynamics of the excited states of curcumin in solution. *J. Phys. Chem. B* **2010**, *114*, 12129−12143.